Research Article

Li Min, Liu Hongbo*, Xie Rongyuan*, Che Xiaorui, Liu Ying, Xu Hao, Zhang Caidong, and Tian Zhiqiang

Investigation of the liquidus temperature calculation method for medium manganese steel

https://doi.org/10.1515/htmp-2022-0285
received May 23, 2023; accepted August 14, 2023

Abstract: The liquidus temperature and temperature drop coefficients of medium manganese steel were systematically studied using Factsage and differential scanning calorimetry (DSC) experiments. The results indicated that the temperature drop coefficients of C, Mn, Cr, Si, and Al were complex, while the coefficients of Mo, V, and Nb were of a constant value. Based on the temperature drop coefficients, the empirical formula for calculating the liquidus temperature of medium manganese steel was established. The liquidus temperature calculated using the empirical formula was 1422.7°C, while that obtained by the DSC experiment was 1422.9°C. By comparison with different calculation formulas, the liquidus temperature obtained from the formula that was constructed in this study was much closer to the experiment one, indicating the high accuracy of the empirical formula in predicting the liquidus temperature of medium manganese steel.

Keywords: liquidus temperature, temperature drop coefficients, DSC, medium manganese steel

*** Corresponding author: Liu Hongbo,** Materials Technology Research Institute, HBIS Group, Shijiazhuang, Hebei, 050000, China, e-mail: ustbliuhongbo@163.com
*** Corresponding author: Xie Rongyuan**, HBIS Digital Technology Co, Ltd, Shijiazhuang, Hebei, 050000, China, e-mail: ncepuxierongyuan@163.com
Li Min, Che Xiaorui, Liu Ying, Zhang Caidong, Tian Zhiqiang: Materials Technology Research Institute, HBIS Group, Shijiazhuang, Hebei, 050000, China
Xu Hao: National Engineering Research Center for Advanced Rolling and Intelligent Manufacturing, University of Science and Technology Beijing, Beijing, 100083, China

1 Introduction

Medium manganese steel, with excellent wear resistance, has been widely used in mining machinery of wear-resistant lining boards [1–3]. However, serious shrinkage cavity and shrinkage porosity defects occur frequently in the production process of the steel [4] when high C [5,6] and high Mn [7] contents are present in the steel. In addition, other alloying elements such as Cr [8] are also added. Therefore, the liquidus temperature of medium manganese steel must be quite different from that of conventional steel. Significant progress has been achieved in the research of the microscopic structure [9,10], heat treatment process [11–13], rolling process [14], and wear performance [15,16] of medium manganese steel; however, the study on liquidus temperature is rarely reported.

Liquidus temperature plays a vital role during the solidification process of steel, which is closely related to the microstructure evolution and solidification quality [17]. In the steelmaking process, the confirmation of tapping temperature is based on the liquidus temperature. An appropriate liquidus temperature can not only ensure the running of the pouring process but also can improve the quality of the billet significantly [18]. At present, experimental methods including the differential thermal analysis (DTA) [19–22], differential scanning calorimetry (DSC) [23–26], thermodynamic software calculation method [22], and empirical formula method [27–30] are often adopted to determine the liquidus temperature of steel. Hamada and Karjalainen [20] investigated the liquidus temperature of Fe–22Mn–0.6C high manganese TWIP steel by DTA measurement and found that the liquidus temperature was 1378°C. Zinke et al. [21] also used DTA and reported the liquidus temperature of Fe–17.8Mn–0.59C–1.33Al–0.22Si steel to be 1,416°C. In order to reduce the experimental errors caused by Mn volatilization during the test and improve the reliability of the results, Zhuang et al. [19] found that the liquidus temperatures of Fe–20Mn–0.75C–1.5Al–0.05Si and Fe–10Mn–0.5C–1.5Al steels were 1406.5 and 1,466°C, respectively, by using the improved DTA equipment. The results obtained by DTA or DSC experiments are accurate; however, the experimental process is expensive and time-consuming, which is not suitable for industrial field production. In addition, some thermodynamic software such as Factsage and Thermo-calc [26,31] can also be used to calculate the liquidus temperature. Pierer et al. [31] pointed out that the liquidus temperature of Fe–25Mn–0.5C–1Al steel calculated with Thermo-calc was 1,411°C, which was lower than that of conventional steel. Because of convenience, the empirical formula method [27–29] was widely adopted during the production process. In this method, the temperature drop coefficients of the composition need to be calculated and then the liquidus temperature can be obtained by the linear sum of the temperature drop coefficients [30]. It should be noted that the temperature drop coefficients of different elements vary, and even the temperature drop coefficients of the same element also varied greatly under different steel components. It was reported that in some steels, the temperature drop coefficients are not independent but shared.

During the past few decades, some formulas have been constructed to predict the liquidus temperature. However, the vast majority of them were applicable to infinitely dilute solutions. But, high alloy content steel such as medium manganese steel does not belong to the category of dilute solution. Thus, these formulas cannot predict the liquidus temperature of high alloy content steels effectively.

Fast and accurate prediction of the liquidus temperature of high alloy content steels is of great significance to the casting temperature of ingot casting and continuous casting, which will eventually affect the quality and yield of the casting billet. Therefore, in the current study, the empirical formula that can effectively determine the liquidus temperature of medium manganese steel was constructed. The results obtained by the formula were in good agreement with the DTA/DSC experiment results. Compared with other formulae, the empirical formulae in this study can effectively predict the liquidus temperature of medium manganese steel. The present study provides theoretical guidance for industrial production, especially for the development of a continuous casting process of medium manganese. Besides, it also provides experience and reference for the accurate prediction of liquidus temperature of other high alloy steels.

2 Materials and methods

2.1 Materials

The ingot of medium manganese steel was fabricated in the ZGJ0.05–100–25 50 kg capacity vacuum induction furnace where the maximum temperature can reach 1,700°C, and the limit vacuum degree is 6.67×10^{-3} Pa. In addition, the ingot was manufactured from commercial pure materials and cast using a cast-iron mold in a vacuum. After the solidification was completed, the riser was removed from the ingot, and the specimens used in ICP and DSC experiments were cut longitudinally at the same position as the ingot. The chip samples of about 5 g were drilled from the specimens for the ICP test. The chemical composition of the experimental steel is given in Table 1.

2.2 DSC test

The liquidus temperature can be determined accurately using DSC. It shows exothermic and endothermic peaks according to the phase transformation of the sample during heating or cooling. The size of the samples in DSC was 3 mm × 2 mm and the weight was approximately 10 mg. The equipment used in this study was NETZSCH STA 449 F5, where the maximum heating temperature can reach 1,800°C, and the range of heating rates can be controlled from 0.001 to $50°C\cdot min^{-1}$. Besides, the measurements were conducted in an inert atmosphere of pure argon with the flow rate maintained at $50\ ml\cdot min^{-1}$. In order to shorten the duration of measurement, the samples were first heated from room temperature to 1,200°C at a heating rate of $50\ K\cdot min^{-1}$. Then, after 30 min of preservation, the samples were continued to be heated above the liquidus temperature to 1,550°C with heating rates of 5, 10, and $15°C\cdot min^{-1}$, respectively. Finally, the temperature was reduced to room temperature at a rate of $50°C\cdot min^{-1}$. The liquidus temperature can be obtained according to the characteristic exothermic peak in the heating process of the steel.

2.3 Calculation using Factsage

The empirical formula method is based on the Fe–I phase diagram. The general formula is shown as follows [32]:

$$T_{\mathrm{liq}} = M_{\mathrm{Fe}} - \sum \Delta t_i^{(1\%)} \cdot \omega_i - 6. \tag{1}$$

where T_{liq} is the liquidus temperature (°C), M_{Fe} is the melting point of pure iron, which is usually selected as

Table 1: Composition of high-carbon medium manganese steel (wt%)

Element	C	Si	Mn	Cr	Mo	Nb	V	Alt
Content	0.95	0.20	8.5	2.1	0.32	0.035	0.065	0.01

1,536–1,539°C, ω_i is the mass fraction of the alloying element, and $t_i^{1\%}$ is the temperature drop coefficient, representing the changes in the liquidus temperature when the element i increased 1%. The effect of gases such as nitrogen, oxygen, and hydrogen on the liquidus temperature is determined at −6°C. The effect of the composition of medium manganese steel on the liquidus temperature was calculated using the thermodynamic software Factsage8.0. During the calculation, the "Equilib" model was selected, and the "FS stel" was selected from data research. Then, the chemical composition was input into the software, and then select IL (equilibrium cooling) to run the program; finally, the precipitation at different temperatures was obtained. The temperature when the solid phase started to precipitate from the liquids was defined as the liquidus temperature. Figure 1 shows the precipitates during the solidification process of Fe–0.95C–8.5Mn–2.1Cr–0.32Mo–0.035Nb–0.065V–0.01Al steel. It can be seen the liquidus temperature is determined as 1422.9°C. According to the calculation results, the temperature drop coefficients ($t_i^{1\%}$) can also be calculated. The empirical formula for calculating the liquidus temperature can be obtained by the linear sum of the coefficients.

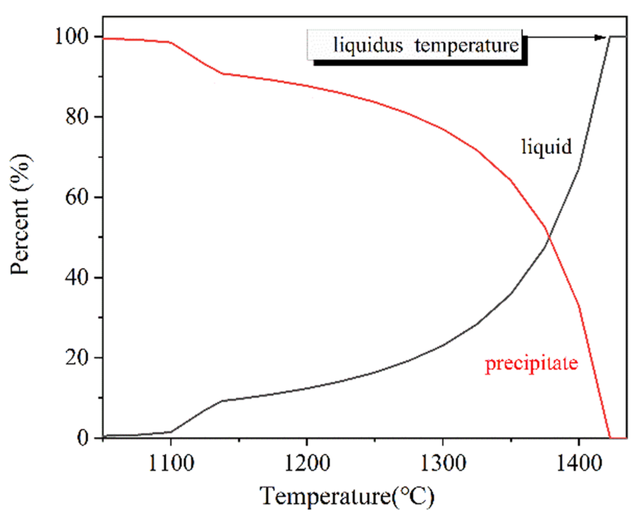

Figure 1: The precipitates during the solidification process of Fe–0.95C–8.5Mn–2.1Cr–0.32Mo–0.035Nb–0.065V–0.01Al steel.

3 Results

3.1 Effect of C on the liquidus temperature

Generally, the increase of C will significantly decrease the liquidus temperature of steel [28]. In this study, the influence of C on the liquidus temperature of medium manganese steel was studied with Factsage8.0. In order to ensure the accuracy and adaptability of the calculation results, the calculation was carried out in a wider range of C content. The results are shown in Table 2. It can be seen that when the content of C increased from 0 to 1.1%, the liquidus temperature of the medium manganese steel decreased from 1478.62 to 1413.12°C. In addition, the temperature drop coefficients also dropped from 91 to 67.82. Other scholars [28,29,33] pointed out the relationship between the liquidus temperature and the C content was linear, which was quite different from the results in this study. The traditional empirical formula was not applicable to predict the liquidus temperature of the medium manganese steel.

Table 2: The liquidus temperature and temperature drop coefficients with different C contents of the medium manganese steel

ω_C (wt%)	Fe–(0–1.1) C–8.5Mn–0.2Si–2.1Cr–0.01Al0.035Nb–0.065V–0.32Mo		ω_C (wt%)	Fe–(0–1.1) C–8.5Mn–0.2Si–2.1Cr–0.01Al0.035Nb–0.065V–0.32Mo	
	T_{liq} (°C)	$\Delta t_c^{1\%}$		T_{liq} (°C)	$\Delta t_c^{1\%}$
0.1	1478.62	91	0.9	1426.15	68.41
0.2	1470.06	88.3	0.92	1424.87	68.32
0.3	1463.12	82	0.94	1423.58	68.23
0.4	1457.13	76.48	0.95	1422.93	68.2
0.5	1451.09	73.26	0.96	1422.29	68.16
0.6	1444.98	71.23	0.98	1420.99	68.09
0.7	1438.8	69.89	1.00	1419.69	68.03
0.8	1432.52	69	1.02	1418.38	67.98
0.82	1431.26	68.85	1.04	1417.07	67.93
0.84	1429.99	68.73	1.06	1415.76	67.89
0.86	1428.71	68.62	1.08	1414.44	67.85
0.88	1427.44	68.5	1.1	1413.12	67.82

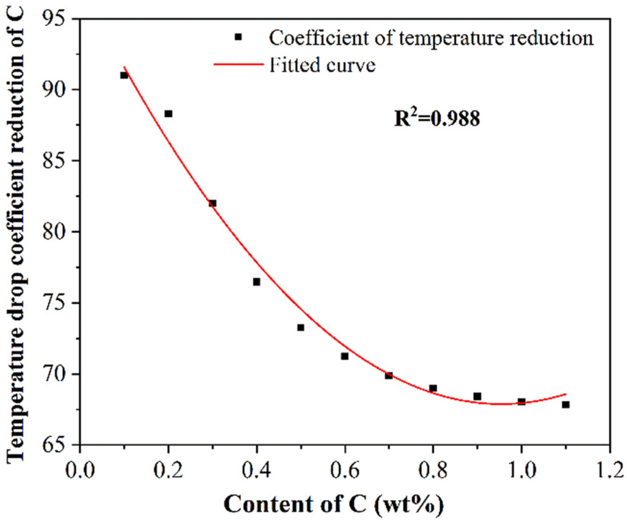

Figure 2: Relationship between the temperature drop coefficients and the C content.

Table 3: The liquidus temperature and temperature drop coefficients with different Mn contents of the medium manganese steel

ω_{Mn} (wt%)	Fe–0.95C–(7–10) Mn–0.2Si–2.1Cr–0.035Nb–0.065V–0.32Mo–0.01Al	
	T_{liq} (°C)	$\Delta t_{Mn}^{1\%}$
7	1428.49	3.66
7.25	1427.57	3.66
7.5	1426.64	3.66
7.75	1425.72	3.66
8	1424.79	3.67
8.25	1423.86	3.67
8.5	1422.93	3.67
8.75	1422.00	3.67
9	1421.08	3.67
9.25	1420.15	3.67
9.5	1419.22	3.67
10	1417.35	3.68

The temperature drop coefficients of C were fitted, as shown in Figure 2. The relationship between coefficients and content conforms to the quadratic distribution, and the fitting degree R^2 = 0.989, indicating that the results are reliable. The formula is shown in equation (2):

$$\Delta t_{C}^{1\%} = 32.52[\%C]^2 - 62.02[\%C] + 97.45. \quad (2)$$

3.2 Effect of Mn on the liquidus temperature

To date, studies on the influence of Mn on the liquidus temperature are rare. The content of Mn in medium manganese steel is much higher than that of conventional steel [34]. Therefore, it is of significance to study the effect of Mn on the liquidus temperature. Figure 3 shows the liquidus temperature and temperature drop coefficients with different contents of Mn. It was found that when the Mn content Mn increased from 7 to 10 wt%, the liquidus temperature decreased almost linearly from 1428.49 to 1417.35°C. Besides, the temperature drop coefficients of Mn were almost constant at around 3.67 (Table 3).

Liu et al. [35] investigated the liquidus temperature of Fe–Mn–C–Al TWIP steels and found that the influence of Mn on the liquidus temperature was closely related to the C content. Whether a similar phenomenon existed in the medium manganese steel needs to be verified. Therefore, the influence of Mn on the liquidus temperature and temperature drop coefficients with different C contents was investigated. The results are shown in Table 4. It was found that when the C content increased from 0.8 to 1.1 wt%, the coefficients decreased from 3.75 to 3.58. Although the temperature drop coefficients of Mn were lower than that of C, considering the Mn content in the medium manganese steel was much higher than C, the influence of Mn on the liquidus temperature cannot be ignored.

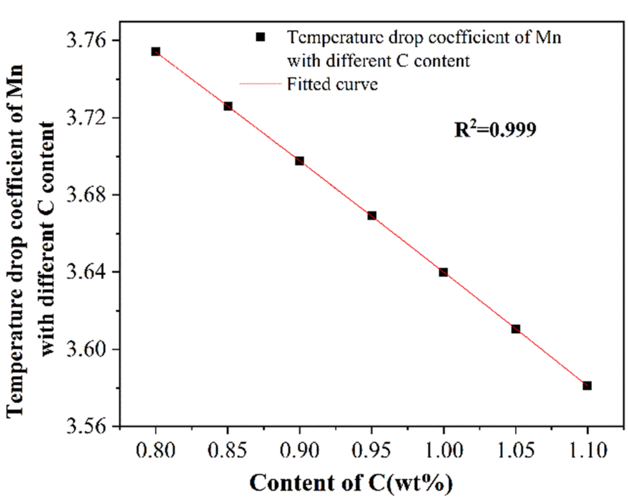

Figure 3: Relationship between the temperature drop coefficients of Mn with different C contents.

The coefficients of Mn with different C contents were fitted. As shown in Figure 3, the variation of the curve is in agreement with the binary polynomial, as shown in equation (3):

$$\Delta t_{Mn}^{1\%} = -0.07[\%C]^2 - 0.45[\%C] + 4.16. \quad (3)$$

The fitting degree R^2 = 0.999, indicating the reliability of the results.

Table 4: The liquidus temperature and temperature drop coefficients of Mn with different C contents of the medium manganese steel

ω_C (wt%)	T_{liq} (°C)		$\Delta t_{Mn}^{1\%}$
	Fe–(0.8–1.1) C–0.2Si–2.1Cr–0.035Nb–0.065V–0.32Mo–0.01Al	Fe–(0.8–1.1) C–8.5Mn–0.2Si–2.1Cr–0.035Nb–0.065V–0.32Mo–0.01Al	
0.8	1464.43	1432.52	3.75
0.85	1461.02	1429.35	3.73
0.9	1457.58	1426.15	3.70
0.95	1454.12	1422.93	3.67
1.00	1450.63	1419.69	3.64
1.05	1447.11	1416.42	3.61
1.10	1443.56	1413.12	3.58

Table 5: The liquidus temperature and temperature drop coefficients with different Cr contents of the medium manganese steel

ω_{Cr} (wt%)	Fe–0.95C–8.5Mn–(1–3) Cr–0.035Nb–0.065V–0.2Si–0.32Mo–0.01Al	
	T_{liq} (°C)	$\Delta t_{Cr}^{1\%}$
0	1426.36	
1.0	1424.8	1.56
1.2	1424.47	1.57
1.4	1424.14	1.59
1.6	1423.8	1.60
1.8	1423.46	1.61
2.0	1423.11	1.63
2.2	1422.76	1.64
2.4	1422.4	1.65
2.6	1422.04	1.66
2.8	1421.67	1.67

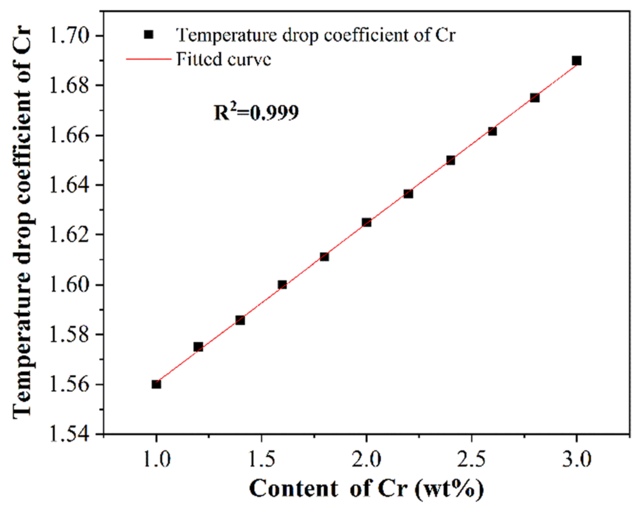

Figure 4: Relationship between the temperature drop coefficients and the Cr content.

3.3 Effect of Cr on the liquidus temperature

An appropriate amount of Cr element added to the steel can improve the mechanical properties of steel effectively [8]. The content of Cr in the medium manganese steel was about 2%, which was lower than that of Mn and much higher than that of C. Therefore, it is of great significance to systematically study the effect of Cr on the liquidus temperature of the medium manganese steel. The liquidus temperature and temperature drop coefficients with different Cr contents were calculated. As shown in Table 5, when the Cr increased from 1 to 3%, the liquidus temperature decreased from 1487.7 to 1422.3°C. Besides, the coefficients of Cr were not constant and it increased from 1.56 to 1.69; although the degree is small, it cannot be neglected. The coefficients of Cr were fitted, as shown in Figure 4. The results demonstrated that the relationship between coefficient and content of Cr is in agreement with linear changes; the fitting degree $R^2 = 0.999$, indicating that the fitting degree was reliable.

$$\Delta t_{Cr}^{1\%} = 1.50 + 0.06[\%Cr]. \tag{4}$$

3.4 Effect of Al on the liquidus temperature

The addition of Al can stabilize and expand the volume fraction of the α phase [8]. However, excessive Al will generate work hardening and deteriorate the strength and ductility of the steel [36,37]. The content of Al in medium manganese steel is lower than 0.01%; therefore, in order to ensure the applicability of the calculation results, the liquidus temperature and temperature drop coefficients with different Al contents were investigated in a wider range. The calculation results are shown in Table 6. It was found that the effect of Al on the liquidus temperature

Table 6: The liquidus temperature and temperature drop coefficients with different Al contents of the medium manganese steel

ω_{Al} (wt%)	Fe–(0–1.1) C–8.5Mn–0.2Si–2.1Cr–0.01Al0.035Nb–0.065V–0.32Mo		ω_{Al} (wt%)	Fe–(0–1.1) C–8.5Mn–0.2Si–2.1Cr–0.01Al0.035Nb–0.065V–0.32Mo	
	T_{liq} (°C)	$\Delta t_{Al}^{1\%}$		T_{liq} (°C)	$\Delta t_{Al}^{1\%}$
0.01	1422.93	−1.00	0.9	1423.09	−0.19
0.02	1422.95	−1.50	1.0	1422.98	−0.06
0.03	1422.96	−1.33	1.1	1422.84	0.07
0.04	1422.98	−1.50	1.2	1422.68	0.20
0.05	1422.99	−1.40	1.3	1422.51	0.32
0.06	1423.01	−1.50	1.4	1422.31	0.44
0.07	1423.02	−1.43	1.5	1422.1	0.55
0.08	1423.03	−1.38	1.6	1421.86	0.66
0.09	1423.05	−1.44	1.7	1421.71	0.71
0.1	1423.06	−1.40	1.8	1422.25	0.37
0.12	1423.08	−1.33	1.9	1422.77	0.08
0.14	1423.1	−1.29	2.0	1423.25	−0.17
0.16	1423.13	−1.31	2.1	1423.71	−0.38
0.18	1423.15	−1.28	2.2	1424.13	−0.55
0.2	1423.16	−1.20	2.3	1424.54	−0.70
0.3	1423.24	−1.07	2.4	1424.91	−0.83
0.4	1423.28	−0.90	2.5	1425.27	−0.94
0.5	1423.29	−0.74	3.0	1426.7	−1.26
0.6	1423.28	−0.60	3.5	1427.66	−1.35
0.7	1423.24	−0.46	4.0	1428.2	−1.32
0.8	1423.18	−0.33			

was complex. When the content of Al increased from 0.01 to 0.5%, the liquidus temperature increased from 1422.93 to 1423.29°C. However, as the Al continued to increase to 1.7%, the liquidus temperature decreased to 1421.71°C. When the Al further increased to 4%, the liquidus temperature again increased to 1428.2°C. It can be seen that when the Al content was lower than 1.7%, the coefficients increased with the increase in Al. However, when the Al content was between 1.8 and 3.5%, the coefficients decreased with an increase in Al. When the content of Al exceeded 4.0%, the coefficients showed again an increasing tendency. Generally speaking, the liquidus temperature increased with the increase in the Al content in conventional steel [30]. However, the calculation results proved that this relationship did not apply to medium manganese steel. The reason that caused this phenomenon is not clear at present. It was speculated that it may be related to the transformation of the structure in medium manganese steel, which still needs to be further confirmed. To reveal the effect of Al on the liquidus temperature of the medium manganese steel, the temperature drop coefficients with various Al contents were fitted, and the results are shown in Figure 5 and equations (5) and (6):

$$\text{Al:0–1.7\%} \quad \Delta t_{Al}^{1\%} = -1.48 + 1.53[\%Al] - 0.12[\%Al]^2, \quad (5)$$

$$\text{Al:1.7–4.0\%} \quad \Delta t_{Al}^{1\%} = 6.82 - 4.91[\%Al] + 0.73[\%Al]^2. \quad (6)$$

The fitting degree R^2 = 0.978 and 0.982, indicating the reliability of the results.

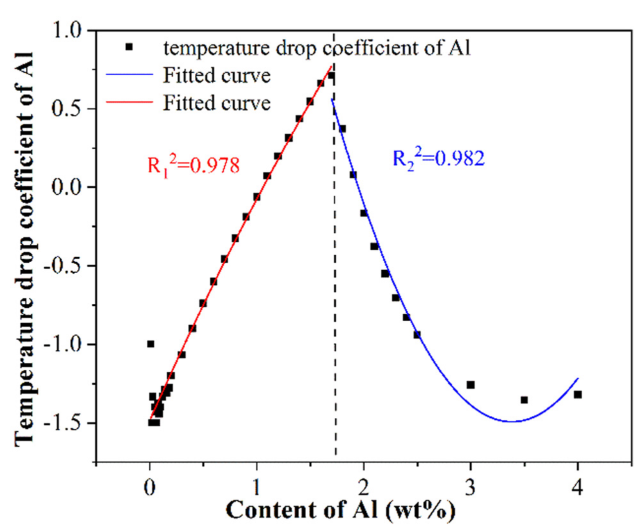

Figure 5: Relationship between the temperature drop coefficients and the Al content.

3.5 Effect of Si on the liquidus temperature

The effect of Si added to the medium manganese steel is similar to that of Al [8]. Si is also one of the ferrite-stable elements. The formation of carbides will be inhibited when appropriate Si is added to the medium manganese steel [38]. The liquidus temperature and temperature drop coefficients were calculated with the Si content ranging from 0 to 4.0%. The results are shown in Table 7. It can be seen that the liquidus temperature decreased from 1429.01 to 1352.26°C and the coefficients decreased from 30.8 to 19.2. The temperature drop coefficients of Si were fitted. As shown in Figure 6 and equation (7), the relationship between the coefficients and the Si content was in accordance with the univariate quadratic distribution:

$$\Delta t_{\mathrm{Si}}^{1\%} = 31.50 - 5.78[\%\mathrm{Si}] + 068[\%\mathrm{Si}]^2. \quad (7)$$

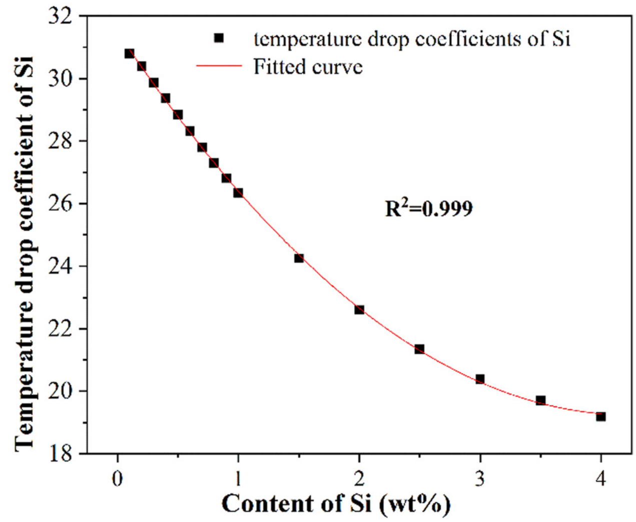

Figure 6: Relationship between the temperature drop coefficients and the content of Si.

3.6 Effect of other elements on the liquidus temperature

Other alloying elements such as Mo, V, and Nb were also added to the medium manganese steel [39,40], which can combine with other elements to form nano-scale precipitates and strengthen the second phase of steel, thus refining the grain, and finally, the strength of the steel can be improved by maintaining certain plasticity [41,42]. Considering that the contents of Mo, V, and Nb were less, the liquidus temperature and temperature drop coefficients were investigated in the range of 0–1, 0–0.1, and 0–0.1%, respectively. As shown in Tables 8–10, when the Mo, V, and Nb contents increased, the liquidus temperature decreased almost linearly. However, the temperature drop coefficients have no obvious changes. Because of the low content of Mo, V, and Nb in medium manganese steel, the coefficients were regarded to be constant and were equal to 4, 4, and 6, respectively.

Table 7: Theliquidus temperature and the temperature drop coefficients with different Si contents of the medium manganese steel

ω_{Si} (wt%)	Fe–0.95C–8.5Mn–(0–1) Si–2.1Cr–0.035Nb–0.065V–0.32Mo–0.01Al	
	T_{liq} (°C)	$\Delta t_{\mathrm{Si}}^{1\%}$
0	1429.01	—
0.1	1425.93	30.80
0.2	1422.93	30.40
0.3	1420.05	29.87
0.4	1417.26	29.38
0.5	1414.59	28.84
06	1412.02	28.32
0.7	1409.55	27.80
0.8	1407.17	27.30
0.9	1404.88	26.81
1.0	1402.67	26.34
1.5	1392.64	24.25
2.0	1383.81	22.6
2.5	1375.66	21.34
3.0	1367.84	20.39
3.5	1360.09	19.69
4.0	1352.26	19.19

Table 8: Theliquidus temperature and temperature drop coefficients with different Mo contents of the medium manganese steel

ω_{Mo} (wt%)	Fe–0.95C–8.5Mn–0.2Si–2.1Cr–0.035Nb–0.065V–(0–1) Mo–0.01Al	
	T_{liq} (°C)	$\Delta t_{\mathrm{Mo}}^{1\%}$
0	1424.2	—
0.1	1423.81	3.90
0.2	1423.41	3.95
0.3	1423.01	3.97
0.4	1422.62	3.95
0.5	1422.22	3.96
0.6	1421.82	3.97
0.7	1421.42	3.97
0.8	1421.02	3.98
0.9	1420.61	3.99
1.0	1420.21	3.99

Table 9: The liquidus temperature and temperature drop coefficients with different V contents of the medium manganese steel

ω_V (wt%)	Fe–0.95C–8.5Mn–0.2Si–2.1Cr–0.035Nb–(0–0.1) V–0.32Mo–0.01Al	
	T_{liq} (°C)	$\Delta t_V^{1\%}$
0	1423.19	—
0.01	1423.15	4
0.02	1423.11	4
0.03	1423.07	4
0.04	1423.03	4
0.05	1422.99	4
0.06	1422.95	4
0.07	1422.91	4
0.08	1422.87	4
0.09	1422.84	3.89
0.1	1422.8	3.90

3.7 The empirical formula of the liquidus temperature of medium manganese steel

The influence of C, Mn, Cr, Al, Si, Mo, V, and Nb on the liquidus temperature and temperature drop coefficients are calculated in Sections 3.1–3.6. Then, the formula to calculate the liquidus temperature of the medium manganese steel can be obtained by the linear sum of these coefficients. It should be noted that the formula can be obtained in the sections according to the Al content. When the Al content ranged from 0 to 1.7%, the liquidus temperature can be obtained as follows:

Table 10: The liquidus temperature and temperature drop coefficients with different Nb contents of the medium manganese steel

ω_{Nb} (wt%)	Fe–0.95C–8.5Mn–0.2Si–2.1Cr–(0–0.1) Nb–0.065V–0.32Mo–0.01Al	
	T_{liq} (°C)	$\Delta t_{Nb}^{1\%}$
0	1423.15	—
0.01	1423.09	6.0
0.02	1423.03	6.0
0.03	1422.97	6.0
0.04	1422.9	6.25
0.05	1422.84	6.20
0.06	1422.78	6.17
0.07	1422.71	6.29
0.08	1422.65	6.25
0.09	1422.59	6.22
0.1	1422.52	6.30

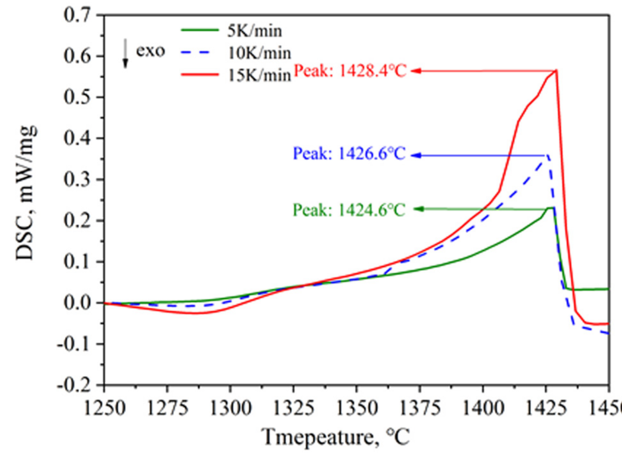

Figure 7: Liquidus temperatures at different heating rates.

$$
\begin{aligned}
T_{liq} = {} & 1,538 - 32.52[\%C]^3 + 62.02[\%C]^2 - 97.45[\%C] \\
& - 0.06[\%Cr]^2 - 1.50[\%Cr] + 0.07[\%C]^2 \\
& \times [\%Mn] + 0.45[\%C] \times [\%Mn] - 4.16[\%Mn] \\
& - 31.50[\%Si] + 5.78[\%Si]^2 - 0.68[\%Si]^3 \\
& + 0.12[\%Al]^3 - 1.53[\%Al]^2 + 1.48[\%Al] \\
& - 4[\%Mo] - 4[\%V] - 6[\%Nb] - 6.
\end{aligned} \quad (8)
$$

Similarly, when the Al content was 1.7–4.0%, the liquidus temperature can be obtained as follows:

$$
\begin{aligned}
T_{liq} = {} & 1538 - 32.52[\%C]^3 + 62.02[\%C]^2 - 97.45[\%C] \\
& - 0.06[\%Cr]^2 - 1.50[\%Cr] + 0.07[\%C]^2 \\
& \times [\%Mn] + 0.45[\%C] \times [\%Mn] - 4.16[\%Mn] \\
& - 31.50[\%Si] + 5.78[\%Si]^2 - 0.68[\%Si]^3 \\
& - 0.73[\%Al]^3 + 4.91[\%Al]^2 - 6.82[\%Al] \\
& - 4[\%Mo] - 4[\%V] - 6[\%Nb] - 6.
\end{aligned} \quad (9)
$$

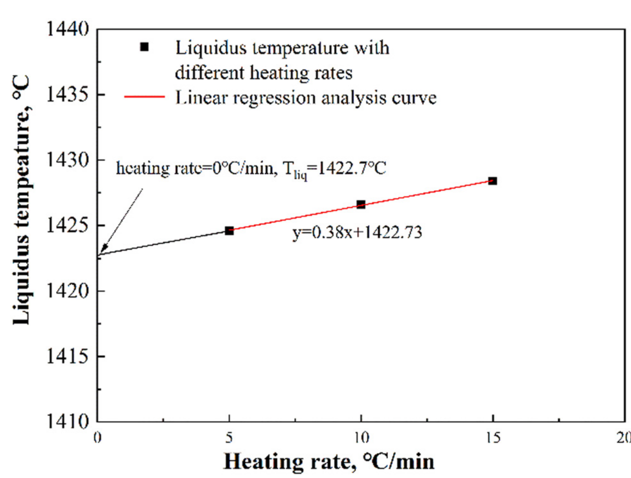

Figure 8: Linear regression analysis of liquidus temperatures.

Table 11: Liquidus temperatures obtained by experiments and the empirical formula

Sample	Composition (wt%)				Liquidus temperature (°C)		Errors
	C	Mn	Al	Si	Results by DTA/DSC	Results by empirical formula	
1	0.59	17.8	1.33	0.22	1,416	1412.41	−3.59
2	0.75	20	1.5	0.05	1406.49	1401.04	−5.45.
3	0.79	13.62	—	0.39	1,419	1414.02	−4.98
4	0.8	12.95	—	0.34	1,422	1417.38	−4.62
5	0.05	19.64	3.47	2.44	1402.68	1397.65	−5.03
6	0.38	25.64	4.12	2.11	1354.9	1356.2	1.30
7	0.38	25.1	3.53	2.78	1346.5	1348.76	2.26
8	0.4	22	—	—	1,405	1412.55	7.55

4 Discussion

4.1 Verification of the results calculated with Factsage

Figure 7 shows the DSC curves during the heating process of the medium manganese steel at heating rates of 5, 10, and 15 K·min^{-1}. The exothermic peak on the DSC curves is considered to be the liquidus temperature of the steel. Therefore, the liquidus temperatures at different heating rates were 1428.4, 1426.6, and 1424.6°C, respectively. That is, the liquidus temperature increased when the heating rates increased. It should be noted that there was a linear relationship between the liquidus temperature and heating rate. Thus, the liquidus temperature of medium manganese steel at a heating rate of 0 K·min^{-1} was 1422.7°C, which can be seen in Figure 8. It should be noted that the liquidus temperature calculated with Factsage was 1422.9°C. The error between the DSC experimental results and the calculated results was within 1%, indicating the accuracy and reliability of the calculated results using Factsage.

Table 12: Different empirical formulae for calculating liquidus temperatures

Number	Empirical formulae
1 [44]	T_{liq} = 1,539–70[%C]–8[%Si]–5[%Mn]–30[%P]–25[%S]–[%Cu]–4[Ni%]–1.5[%Cr]
2 [28]	T_{liq} = 1,491–36.33[%C] + 61.9[%C]^2–17.10[%Si]–3.32[%Mn]–27.07[%P] – 30.40[%S]–2.61[Cr%]–3.25[Mo%]–1.60[%Ni]–1.7[%Cu]–10.17[%Ti] – 0.86[%Co]–2.11[%W]
3 [44]	T_{liq} = 1,535–73[%C]–3[%Mn]–12[%Si]–28[%P]–30[%S]– [%Cr]–3 [%Al]
4 [44]	T_{liq} = 1,534–80[%C]–4[%Mn]–14[%Si]–35[%P]–1.4 [%Cr]–3.4[%Al]
5 [33]	T_{liq} = 1,536–83[%C]–31.5[%S]–32[%P]–5[%Mn + Cu]–7.8[%Si]–3.6[%Al] – 1.5[%Cr]–2[%Mo]–4[%Ni]–18[%Ti]–2[%V]
6 [27]	T_{liq} = 1,539–100.3[%C] + 22.41[%C]^2–3.55[%Si] + 0.64[%Si]^2–5.82[%Mn]–0.3[%Mn]^2–1.59[%Cr] + 0.007[%Cr]^2–[%Mo]–4.18[%Ni]–0.01[%Ni]–2.42[%Cu]
7 [29]	T_{liq} = 1,538–31.15[%C]^2–62.645–[%C]–0.609[%Si]^2–2.0678[%Si] + 0.0674[%Mn]^2–5.3464[%Mn]–20[%P]^2–9[%P] + 1.7724[%S]^2 – 24.755[%S]–1.1159[%Nb]–15.3326[%Nb] + 0.0758[%Ca]^2–3.1313[%Ca] – 0.0379[%Ni]–5.2917[%Ni]–0.6818[%Cu]^2–2.5955[%Cu]–0.0214[%Mo]^2 – 3.2214[%Mo]–0.0359 [%Cr]^2–1.1402[%Cr] + 1.791.
8 [44]	T_{liq} = 1,536–83.9[%C]–10[%C]2–12.6[%Si]–54[%Mn] – 4.6[%Cu]–5.1[%Ni]–1.5[%Cr] + 33[%Mo] + 30[%P] + 37[%S] + 9.5[%Nb]–0.1
9 [44]	T_{liq} = 1,536–8[%C]–7.6[%Si]–3.9[%Mn]–33.4[%P]–38[%S]–1.3[%Cr]–3.6[%Al]
10[44]	T_{liq} = 1536–251[%C]–12.3[%Si]–6.8[%Mn]–123.4[%P]–183.9[%S]–14[%Cr]–3.6 [%Al]

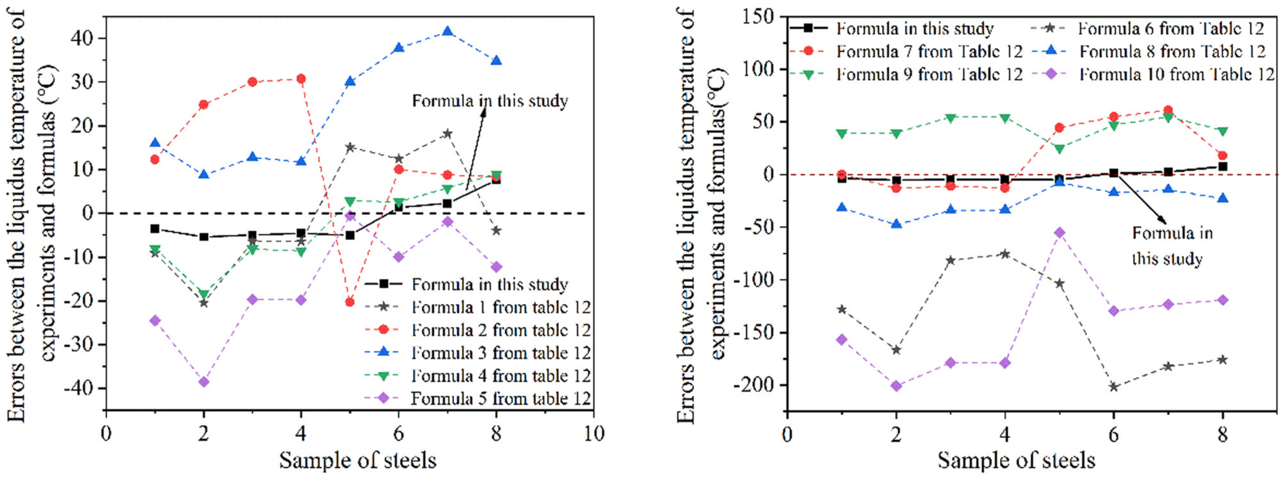

Figure 9: Errors between the liquidus temperature of experiments and formulae.

4.2 Verification of the empirical formula

The liquidus temperatures of the medium manganese steel obtained by DTA or DSC experiments [19,21,43] were investigated, and the results are shown in Table 11. It can be found that the liquidus temperatures calculated by the empirical formula were close to experiment results, and all of the errors were within 8°C. Besides, the different empirical formulas for calculating liquidus temperatures of steel are also given in Table 12. Figure 9 shows the liquidus temperatures obtained by different empirical formulas. On the whole, except for a few examples, most of the results obtained using the empirical formula in the current study were much closer to experiment results, indicating the accuracy and reliability of the formula to predict the liquidus temperature of the medium manganese steel. It should be noted that the composition in the table is only to verify the accuracy and adaptability of the empirical formula. Therefore, although the content of some elements exceeds the limited range of the empirical formula in this study, the calculation results still have reference value.

5 Conclusions

1. The temperature drop coefficients of the medium manganese steel were calculated using Factsage. When the content of C,、Mn,、Cr, and、Si increased, the coefficients of C and Mn increased nonlinearly, and the coefficients of Cr increased linearly, while the coefficient of Si decreased. However, the coefficients of Al were complex when the Al content was lower than 1.7% and the coefficient increased with an increase in Al. When the Al content was between 1.8 and 3.5%, the coefficient decreased with an increase in Al. When the content of Al exceeded 4.0%, the coefficient showed an increasing trend again. Considering the lower contents of Mo, V, and Nb in the medium manganese steel, the temperature drop coefficients were constant and equal to 4, 4, and 6, respectively.
2. The empirical formulae for calculating the liquidus temperature of the medium manganese steel were established by the linear sum of the corresponding temperature drop coefficients. In the current study, when the Al content ranged from 0 to 1.7%, the liquidus temperature can be obtained as

$$\begin{aligned} T_{\text{liq}} = {} & 1{,}538 - 32.52[\%\text{C}]^3 + 62.02[\%\text{C}]^2 - 97.45[\%\text{C}] \\ & - 0.06[\%\text{Cr}]^2 - 1.50[\%\text{Cr}] + 0.07[\%\text{C}]^2 \times [\%\text{Mn}] \\ & + 0.45[\%\text{C}] \times [\%\text{Mn}] - 4.16[\%\text{Mn}] - 31.50[\%\text{Si}] \\ & + 5.78[\%\text{Si}]^2 - 0.68[\%\text{Si}]^3 + 0.12[\%\text{Al}]^3 - 1.53[\%\text{Al}]^2 \\ & + 1.48[\%\text{Al}] - 4[\%\text{Mo}] - 4[\%\text{V}] - 6[\%\text{Nb}] - 6. \end{aligned}$$

When the content of Al was 1.7–4.0%, the liquidus temperature can be calculated as by

$$\begin{aligned} T_{\text{liq}} = {} & 1{,}538 - 32.52[\%\text{C}]^3 + 62.02[\%\text{C}]^2 - 97.45[\%\text{C}] \\ & - 0.06[\%\text{Cr}]^2 - 1.50[\%\text{Cr}] + 0.07[\%\text{C}]^2 \times [\%\text{Mn}] \\ & + 0.45[\%\text{C}] \times [\%\text{Mn}] - 4.16[\%\text{Mn}] - 31.50[\%\text{Si}] \\ & + 5.78[\%\text{Si}]^2 - 0.68[\%\text{Si}]^3 - 0.73[\%\text{Al}]^3 + 4.91[\%\text{Al}]^2 \\ & - 6.82[\%\text{Al}] - 4[\%\text{Mo}] - 4[\%V] - 6[\%\text{Nb}] - 6. \end{aligned}$$

3. The reliability of the empirical formulae to predict the liquidus temperature was verified. The liquidus temperature of the medium manganese steel found by the DSC experiment was 1422.7°C, which was closer to that obtained using the empirical formula. By comparison

with different empirical formulas, the results calculated by the formula in this study were closer to the experimental results, indicating the reliability of the empirical formula in determining the liquidus temperature of the medium manganese steel.

Acknowledgments: The authors gratefully acknowledge the financial support provided by the Natural Science Foundation of Hebei Province (No. E2021318004) and the Central and Local Science and Technology Development Fund Project (No. 216Z1009G).

Funding information: This research was supported by: Natural Science Foundation of Hebei Province (No. E2021318004) as well as Central and Local Science and Technology Development Fund Project (No. 216Z1009G).

Author contributions: Conceptualization, L.Y.; methodology, L.M. and C.X.R.; validation, X.R.Y.; formal analysis, Z.C.D.; investigation, T.Z.Q.; writing – original draft preparation, L.M.; writing – review and editing – L.H.B and L.M.; Supervision, X.H.

Conflict of interest: The authors state no conflict of interest.

Data availability statement: The data presented in this study are available on request from the corresponding author.

References

[1] Song, Y. P., J. P. Xie, Y. M. Zhu, and A. Q. Wang. Effect of RE-modifier on microstructure and mechanical property of high-carbon medium-manganese steel. *Journal of Iron and Steel Research International*, Vol. 9, No. 1, 2002, pp. 36–39.

[2] Sun, R. M., W. H. Xu, C. Y. Wang, J. B. Qiu, and W. Q. Cao. Wear resistant of new type medium manganese high strength martensite steel. *Iron and Steel*, Vol. 12, 2012, pp. 64–70.

[3] Ge, S. R., J. X. Wang, Q. L. Wang, and H. Chen. Self-strengthening wear resistant mechanism and application of medium manganese steel applied for the chute of scraper conveyor. *Journal of China Coal Society*, Vol. 41, No. 9, 2016, pp. 2373–2379.

[4] Wang, D., J. Liu, H. Luo, L. Guo, and H. Zhang. Delaminating defects analysis of continuous casting mid-manganese wear-resistant steel slab. *Baosteel Technology*, 2016, Vol. 7, No. 3, pp. 36–40.

[5] Dou, C., S. Wei, S. I. Anheng, Z. Shen, and S. Liao. Effect of carbon content and heat treatment on microstructure and properties of medium manganese wear-resistant steel. *Foundry Technology*, Vol. 2, 2018, pp. 289–294.

[6] Grajcar, A., E. Kalinowska-Ozgowicz, M. Opiela, B. Grzegorczyk, and K. Golombek. Effects of Mn and Nb on the macro-and microsegregation in high-Mn high-Al content TRIP steels. *Archives of Materials Science and Engineering*, Vol. 49, No. 1, 2011, pp. 5–14.

[7] Chen, J., J. J. Wang, H. Zhang, W. G. Zhang, and C. M. Liu. Evolution of deformation twins with strain rate in a medium-manganese wear-resistant steel Fe–8Mn–1C–1.2Cr–0.2V]. *Journal of Iron and Steel Research International*, Vol. 26, 2019, pp. 983–990.

[8] Ren-bo, S. O., H. U. Wei-feng, Z. H. Nai-peng, L. I. Jia-jia, Z. H. Zhe-rui, and W. A. Yong-jin. Research progress and prospect of Fe– Mn– Al– C medium Mn steels. *Chinese Journal of Engineering*, Vol. 42, No. 7, 2020, pp. 814–828.

[9] Cai, Z. H., H. Ding, X. Xue, J. Jiang, Q. B. Xin, and R. D. K. Misra. Significance of control of austenite stability and three-stage work-hardening behavior of an ultrahigh strength–high ductility combination transformation-induced plasticity steel. *Scripta Materialia*, Vol. 11, 2013, pp. 865–868.

[10] Lee, S., K. Lee, and B. C. De Cooman. Observation of the TWIP + TRIP plasticity-enhancement mechanism in Al-added 6 wt pct medium Mn steel. *Metallurgical and Materials Transactions A*, Vol. 6, 2015, pp. 2356–2363.

[11] Hu, J., W. Cao, C. Wang, H. Dong, and J. Li. Phase transformation behavior of cold rolled 0.1 C–5Mn steel during heating process studied by differential scanning calorimetry. *Materials Science and Engineering: A*, Vol. 636, 2015, pp. 108–116.

[12] Luo, L., W. Li, L. Wang, S. Zhou, and X. Jin. Tensile behaviors and deformation mechanism of a medium Mn-TRIP steel at different temperatures. *Materials Science and Engineering: A*, Vol. 682, 2017, pp. 698–703.

[13] Speer, J. G., D. V. Edmonds, F. C. Rizzo, and D. K. Matlock. Partitioning of carbon from supersaturated plates of ferrite, with application to steel processing and fundamentals of the bainite transformation. *Current Opinion in Solid State and Materials Science*, Vol. 8, No. 3–4, 2004, pp. 219–237.

[14] Wang, J., Q. Wang, X. Zhang, and D. Zhang. Impact and rolling abrasive wear behavior and hardening mechanism for hot-rolled medium-manganese steel. *Journal of Tribology*, Vol. 140, No. 3, 2018, id. 031608.

[15] Luo, K. and B. Bai. Microstructure, mechanical properties and high stress abrasive wear behavior of air-cooled MnCrB cast steels. *Materials & Design (1980-2015)*, Vol. 31, No. 5, 2010, pp. 2510–2516.

[16] Yan, X., J. Hu, H. Yu, C. Wang, and W. Xu. Unraveling the significant role of retained austenite on the dry sliding wear behavior of medium manganese steel. *Wear*, Vol. 476, 2021, id. 203745.

[17] Schaffnit, P., C. Stallybrass, J. Konrad, F. Stein, and M. Weinberg. A Scheil–Gulliver model dedicated to the solidification of steel. *Calphad*, Vol. 48, 2015, pp. 184–188.

[18] Howe, A. A. Estimation of liquids temperatures for steels. *Ironmaking & Steelmaking*, Vol. 3, 1988, pp. 134–142.

[19] Zhuang, C., J. Liu, C. Bernhard, and P. Presoly. Analysis of solidification of high manganese steels using improved differential thermal analysis method. *Journal of Iron and Steel Research, International*, Vol. 22, No. 8, 2015, pp. 709–714.

[20] Hamada, A. S. and L. Karjalainen. Hot ductility behaviour of high-Mn TWIP steels. *Materials Science & Engineering A*, Vol. 3, 2011, pp. 1819–1827.

[21] Keil, D., M. Zinke, and H. Pries. *Investigations on hot cracking of novel high manganese TWIP-steels[M]//Hot Cracking Phenomena in Welds III*, Berlin, Heidelberg: Springer: 2011, pp. 209–223.

[22] Martiník, O., B. Smetana, J. Dobrovská, S. Zlá, M. Kawuloková, K. Gryc, et al. Experimental and theoretical assessment of liquidus, peritectic transformation, and solidus temperatures of laboratory and commercial steel grades. *Journal of Phase Equilibria and Diffusion*, Vol. 40, 2019, pp. 93–103.

[23] Han, Z. B., J. H. Liu, Y. He, K. W. Li, Y. L. Ji, and J. Liu. Determination of the liquidus and solidus temperatures of FeCrAl stainless steel. *International Journal of Minerals Metallurgy & Materials*, Vol. 22, 2015, pp. 1141–1148.

[24] Kousksou, T., A. Jamil, Y. Zeraouli, and J. P. Dumas. Equilibrium liquidus temperatures of binary mixtures from differential scanning calorimetry. *Chemical Engineering Science*, Vol. 62, No. 23, 2007, pp. 6516–6523.

[25] Steiner Petrovič, D., G. Klančnik, M. Pirnat, and J. Medved. Differential scanning calorimetry study of the solidification sequence of austenitic stainless steel. *Journal of Thermal Analysis and Calorimetry*, Vol. 1, 2011, pp. 251–257.

[26] Shen, Y., J. Liu, and H. Xu. Investigation of solidification modes of high Manganese steels. *Materials Science and Technology*, Vol. 4, 2021, pp. 446–457.

[27] Mathew, J. and H. Brody. Solidification and Casting of Metals[C]. *Sheffield Conference*, 1979.

[28] Kagawa, A. and T. Okamoto. Influence of alloying elements on temperature and composition for peritectic reaction in plain carbon steels. *Metal Science Journal*, Vol. 10, 1986, pp. 997–1008.

[29] Wang, X., X. Wang, B. Wang, B. Wang, and Q. Liu. Differential calculation model for liquidus temperature of steel. *Steel Research International*, Vol. 823, 2011, pp. 164–168.

[30] Wu, Y. J., Z. H. Jiang, L. K. Liang, M. Jiang, and Y. Li. Calculation on liquidus temperature of steel. *Gangtie Yanjiu Xuebao (Journal of Iron and Steel Research) (China)*, Vol. 14, 2002, pp. 6–9.

[31] Gigacher, G., R. Pierer, J. Wiener, and C. Bernhard. Metallurgical aspects of casting high-manganese steel grades. *Advanced Engineering Materials*, Vol. 8, No. 11, 2010, pp. 1096–1100.

[32] Won, Y.-M. and B. G. Thomas. Simple model of microsegregation during solidification of steels. *Metallurgical and Materials Transactions A*, Vol. 32, 2001, pp. 1755–1767.

[33] Choudhary, S. K. and A. Ghosh. Mathematical model for prediction of composition of inclusions formed during solidification of liquid steel. *ISIJ International*, Vol. 49, No. 12, 2009, pp. 1819–1827.

[34] Sun, B., H. Aydin, F. Fazeli, and S. Yue. Microstructure evolution of a medium manganese steel during thermomechanical processing. *Metallurgical and Materials Transactions A*, Vol. 47, 2016, pp. 1782–1791.

[35] Liu, H., J. Liu, B. Wu, Y. Shen, Y. He, H. Ding, et al. Effect of Mn and Al contents on hot ductility of high alloy Fe-xMn-C-yAl austenite TWIP steels. *Materials Science and Engineering: A*, Vol. 708, 2017, pp. 360–374.

[36] Cai, Z. H., B. Cai, H. Ding, Y. Chen, and R. D. Misra. Microstructure and deformation behavior of the hot-rolled medium manganese steels with varying aluminum-content. *Materials Science and Engineering: A*, Vol. 676, 2016, pp. 263–270.

[37] Lehnhoff, G., K. Findley, and B. De Cooman. The influence of silicon and aluminum alloying on the lattice parameter and stacking fault energy of austenitic steel. *Scripta Materialia*, Vol. 92, 2014, pp. 19–22.

[38] Heo, Y.-U., Y.-Y. Song, S.-J. Park, H. K. D. H. Bhadeshia, and D. W. Suh. Influence of silicon in low density Fe-C-Mn-Al steel. *Metallurgical and Materials Transactions A*, Vol. 6, 2012, pp. 1731–1735.

[39] Cai, M., Z. Li, Q. Chao, and P. D. Hodgson. A novel Mo and Nb microalloyed medium Mn TRIP steel with maximal ultimate strength and moderate ductility. *Metallurgical and Materials Transactions A*, Vol. 12, 2014, pp. 5624–5634.

[40] Lee, D., J. K. Kim, S. Lee, K. Lee, and B. C. De Cooman. Microstructures and mechanical properties of Ti and Mo micro-alloyed medium Mn steel. *Materials Science and Engineering: A*, Vol. 706, 2017, pp. 1–14.

[41] Lee, S. and B. C. De Cooman. Tensile Behavior of Intercritically Annealed Ultra-Fine Grained 8% Mn Multi-Phase Steel. *Steel Research International*, Vol. 10, 2015, pp. 1170–1178.

[42] Cai, Z. H., H. Ding, H. Kamoutsi, G. N. Haidemenopoulos, and R. D. Misra. Interplay between deformation behavior and mechanical properties of intercritically annealed and tempered medium-manganese transformation-induced plasticity steel. *Materials Science and Engineering: A*, Vol. 654, 2016, pp. 359–367.

[43] Zhung, C. L. Research on metallurgical fundamental and solidification of low carbon TWIP steels abstract[D]. 2014

[44] Liu, H. B. Analysis of Metallurgical Fundamental and Solidification Characteristics of Fe-Mn-C (-Al) TWIP Steel[D]. 2018.